Climb Performance Anomalies in 'Real' Atmospheric Conditions

Timothy T. Takahashi[1]
Arizona State University, Tempe, AZ

András Sóbester[2]
University of Southampton, Southampton, UK

This paper summarizes problems with the classic "constant Mach number" and "constant indicated airspeed" corrections for work-energy-theorem derived climb performance. Expanding upon previous work that demonstrated considerable inaccuracy inherent in the small-angle-approximation formulation for unaccelerated climb, this work documents secondary sources of significant error: the differences between actual atmospheric properties and the "reference standard atmosphere" and the common conflation of constant equivalent airspeed with constant calibrated airspeed climb.

I. Introduction

MOST aircraft design books base aircraft climb performance on the work-energy theorem [1-4], which is a direct byproduct of Newton's second law ($\vec{F} = m\vec{a}$). Aircraft performance engineers apply the work-energy theorem to hold that the theoretical change in kinetic energy of a rigid body may also express itself as a change in elevation or gravitational potential energy. In theory, this theorem is directly useful in deriving the unaccelerated rate-of-climb of an aircraft. In practice, it requires modifications for the manner in which aircraft are actually flown: generally climbing or descending while holding a constant indicated airspeed or a constant Mach number. Because both atmospheric temperature and density lapse with altitude, a climb or descent flown at constant airspeed or Mach number is, in fact, accelerated flight.

In a previous paper [5] Takahashi demonstrated problems inherent in the manner that the work-energy theorem has been applied to estimate aircraft performance. He found that the predicted performance arising from the full equations of motion differ substantially from that predicted by a simplified, work-energy-theorem model; the work-energy-theorem model tends to underestimate actual climb performance by 10 to 25% under typical situations. Thus, precise computing of the climb gradient or the rate-of-climb is requires solution of the general equation of motion. As much as engineers learn early in their eduation that the work-energy-theorem is an exact representation of Newton's second law, the classic work-energy-theorem model that asssumes unaccelerated climb is subject to significant error.

Here, we extend this line of reasoning to consider the implications of the typical constant indicated airspeed or constant Mach number correction to the work-energy-theorem climb rate. The work-energy-theorem climb rate equation formally estimates an unaccelerated climb; handbook correction methods based upon the "Standard Atmosphere" adjust the unaccelerated climb to represent climb at constant airspeed or Mach number.

In this new work we examine three sources of error affecting climb performance prediction that are not accounted for in 'textbook' models: 1) those that arise from the small angle approximation [5], 2) those that are the byproducts of correction factors based upon fundamental attributes of the pressure and density lapse (implied by the standard-atmosphere model) and 3) those that are functions of unrepresentativeness of international standard atmosphere (ISA)

[1] Professor of Practice, Aerospace and Mechanical Engineering, School for Engineering of Matter, Transport & Energy, P.O. Box 876106, Tempe, AZ, 85287. Associate Fellow AIAA.
[2] Associate Professor of Aircraft Engineering, Aeronautics and Astronautics, School of Engineering, Southampton, SO16 7QF, Senior Member AIAA.

model regarding real density, temperature and pressure lapse rates. The reader will see here that the vagaries of actual weather conditions, which impact the pressure, density and temperature lapse rate, indeed materially affect the "classic" climb performance correction factors.

II. Prior Art

A. Fundamentals – Work / Energy Theorem

Newton's Second Law holds that that the rate of change of momentum of a body is directly proportional to the force applied In an environment with no net force imbalance), the sum of kinetic and gravitational potential energy must conserve. These axioms lead us the the famous work-energy theorem:

$$\frac{1}{2}\, m\, V^2 + mgh = const. \tag{1}$$

Nothing in the rest of this paper disputes these fundamental principles.

We hold that the traditional application of these equations to estimate aircraft performance oversimplifies the actual physics, and leads to an imprecise (or even inaccurate) understanding of aircraft flight dynamics.

B. Initial Applications of Work / Energy to Aircraft Performance

The earliest published method to estimate aircraft climb performance may be found in Reference 7, in which DeBothezat states that the rate of climb is a function of the forward flight speed (in terms of true airspeed, *V*tas) and the flight path angle, γ:

$$ROC \propto Vtas \cdot \gamma \tag{2}$$

He goes on to define flight path angle γ as a function of thrust, *T*, aircraft flight weight, *W*, and the lift-to-drag ratio (*L/D*) using the implicit trigonometric relationship tan(γ)≈γ for small angles:

$$\gamma = \frac{T}{W} - \frac{1}{L/D} \tag{3}$$

He assumes that during climb lift must exactly oppose weight (*L*=*W*), thus:

$$\gamma = \frac{T-D}{W} \tag{4}$$

so that he may then apply the work-energy theorem to find the rate-of-climb expressed in-ft/min as:

$$ROC \propto Vtas \cdot \frac{T-D}{W} \tag{5}$$

DeBothezat makes the key assumptions here that are also found in most subsequent texts:

- aerodynamic lift must equal weight; in other work Takahashi [5] demonstrated that this is an oversimplification that introduces significant error (see also Figure 1 from [1] showing that the greater the climb angle the more of the weight is supported by thrust; in the extreme case of a 90 degree climb angle, all of it is).

- the flight path angle may be represented by the work-energy-theorem derived function: *T/W – 1/(L/D)*; in earlier work Takahashi [5] demonstrated that this simplification introduces additional error.

B. The Classic Legacy Textbook Derivation - Anderson

John Anderson's classic performance text [1] has been widely used to teach aerospace engineering students. He begins with a free-body-diagram; see Figure 1. Anderson writes the principal equations of motion as:

$$T - D - W\sin(\gamma) = 0 \qquad (6a)$$

and

$$L - W\cos(\gamma) = 0. \qquad (6b)$$

He then works through a brief derivation that returns us to the classic work-energy relationship:

$$RoC = \frac{excess\ power}{W} \qquad (7)$$

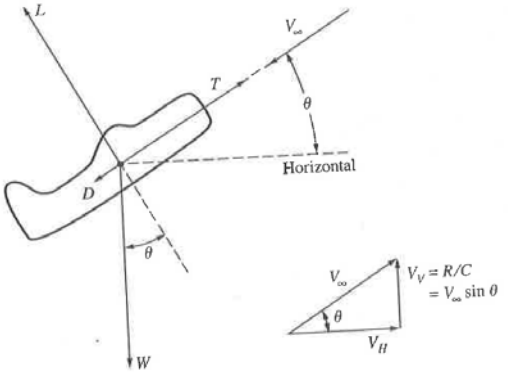

FIGURE 1 – Free Body Diagram after Anderson [1]

Anderson later notes that in steady climbing flight, the lift of the aircraft may be less than the weight because "part of the weight of the airplane is supported by the thrust." [1] Thus, he suggests that the excess power computation be made in such a manner that the dimensional drag of the aircraft accounts for the offset in lift-induced drag due to thrust. He states that the nuance of the derivation are "details … left for a homework problem." But agrees that the exact solution for climb is "unwieldy to solve" because the flight-path-angle (γ) shows up in multiple places within the excess power equation.

C. A More Generalized Approach to Aircraft Performance – Roskam

Roskam's classic performance text [2] includes a free-body-diagram that includes flight path angle (γ) and angle-of-attack (α). He writes the generalized equations of motion as:

$$T\cos(\alpha+\gamma) - D - Wsin(\gamma) = \frac{W}{g}\frac{dV}{dt} \qquad (8a)$$

$$T\sin(\alpha+\gamma) + L - Wcos(\gamma) = \frac{W}{g}V\dot{\gamma} \qquad (8b)$$

Roskam then states that we should simplify the equations of motion for "small angles" and make the substitutions $\sin(\gamma)=\gamma; \cos(\gamma)=1; \sin(\alpha+\gamma)=0; \cos(\alpha+\gamma)=1$ to reduce the equations of motion to the classic form:

$$T - D - \frac{W}{g}\frac{dV}{dt} = W\sin(\gamma) \qquad (9)$$

where lift equals weight (L=W).

D. Industry Reference Formulation with Additional Correction Factors - Blake et al.

Blake [8] mirrors Roskam and replicates the derivation of Equation 9, noting that "the regulatory minimum allowable climb angles specified for takeoff are less than two degrees" and thus $\cos\gamma = 1$ (that is, lift is equal to weight) is an acceptable approximation. He also states that: "the two simplifying assumptions we have made: first, that lift equals weight, and second that the tangent of the climb angle is equal to the sine of the angle, are only acceptable for relatively small angles of climb." Blake further suggests that "for more precise calculations, and especially when calculating climb angles with all engines operating," the engineer should solve the full equations of motion [8]. Recall that

Takahashi[5] demonstrated that this simplification introduces additional error, even when computing climb near the regulatory minimums.

Blake also notes that due to air traffic control and piloting instrumentation convention, pilots tend to fly either: 1) constant indicated airspeed (*IAS*) or calibrated airspeed (*CAS*) climbs and descents or 2) constant Mach number (*M*) climbs and descents. [8]

The 1962 Standard Atmosphere is the foundation for 14 CFR § 25 certified aircraft performance [9][10].

Because the density of the air decreases with an increase in altitude, a climb at constant indicated airspeed requires the aircraft to increase its true airspeed (and hence its kinetic energy) as it ascends. Conversely, during a climb at constant Mach number in a region of the atmosphere where there is a cooling temperature gradient with increasing altitude, the aircraft must slightly decrease its true airspeed (and hence its kinetic energy) as it climbs.

Reference 8 also highlights the need to compute performance during an "accelerated climb." Thus:

$$P_s = \frac{(T-D)\,V}{W} = \frac{dALT}{dt} \approx RoC_{unaccelerated} \tag{10}$$

Of course, the devil is in the details; real aircraft do not fly truly un-accelerated climb profiles. Consequently, Blake [8] estimates the actual rate-of-climb as:

$$RoC = \frac{RoC_{unaccelerated}}{(1+\frac{VdV}{gdh})} \tag{11}$$

As before, this equation infers that the rate-of-climb is linearly proportional to P_s.

Correction factors, based upon the standard atmosphere altitude lapse rate [10], can account for this effect. Thus, Blake [8] presents the small-angle approximation rate-of-climb at a given Mach number and altitude as:

$$RoC(M,ALT) \approx K_{accel} \cdot ROC_{\ unacelerated}(M,ALT) \tag{12}$$

Which when applied to the structure of the 1962 Standard Atmosphere models [10] results in:

$$K_{accel} = \frac{1}{1+.566816 \cdot M^2} \tag{13a}$$

for climb at constant equivalent (*EAS*) airspeed below the tropopause (*ALT* <36,089-ft), and

$$K_{accel} = \frac{1}{1+.7 \cdot M^2} \tag{13b}$$

for climb at constant equivalent (*EAS*) airspeed above the nominal tropopause (*ALT*>36,089-ft).

Because climb at constant indicated airspeed requires the aircraft to accelerate with respect to a fixed frame of reference and increase its kinetic energy as its climbs, less energy remains to influence changes in potential energy. Thus, an aircraft flying a constant indicated airspeed climb will gain altitude slightly more slowly than the basic, un-accelerated equations of motion would predict.

Similarly, the *k*-factors for climb at constant Mach number are:

$$K_{accel} = \frac{1}{1-.133184 \cdot M^2} \tag{13c}$$

for climb below the nominal tropopause (*ALT* <36,089-ft), and

$$K_{accel} = 1 \tag{13d}$$

for climb at constant Mach number above the nominal tropopause (*ALT*>36,089-ft).

In this paper, we question the generality and applicability of these *"K"* factors.

E. Sensitivities of the acceleration factor

Reference 18 adopts a similar acceleration factor approach which presents derivations for the cases of climbing at a constant equivalent or calibrated airspeed or climb at constant Mach number. It also includes a calculation of the ratio of acceleration factors (for both climb and descent) for the constant calibrated and constant equivalent airspeed cases for a range of Mach numbers. The temperature sensitivity of this ratio is considered and they show that the impact of offsetting the standard atmosphere temperature profile by 10% either side. They conclude that conflating the constant equivalent and constant calibrated airspeed climb scenario is safe 'for low-speed' applications (the 10% temperature deviation curves diverge more significantly in the supersonic range). A more extensive analytical study of acceleration factor sensitivities is conducted in Reference 19, taking the constant true airspeed climb case as the baseline and deriving derivatives with respect to a range of variables, including the airspeed, the density lapse rate of the atmosphere. Reference 19 also presents an example (that of a 10,000-lbm jet with a baseline rate of climb of 3,000-ft/min) and it examines the impact of variations in weight in the constant true airspeed and equivalent airspeed case, as well as the effect of variations in the ambient density.

In the context of the observations detailed in Refences 18 and 19, Reference 20 emphasises the importance of solving the complete equations of motion for the general case, for example when, to understand measured performance data, the wind gradients also have to be accounted for.

Throughout our further analysis, we will presume that the air-data system is well calibrated so that we can conflate indicated and calibrated airspeed: $CAS \cong IAS$. At the same time, we will seek to identify how compressibility effects that render calibrated airspeed (*CAS*) somewhat different than equivalent airspeed (*EAS*) will impact these corrections. In addition, we will seek to identify how daily variations in the atmospheric profile (including low altitude temperature inversions and the presence or absence of a true tropopause) influence these correction factors.

III. The Standard Atmosphere Model in contrast to Regional Weather

Recall that the the FAA defines the 1962 U.S. Standard Atmosphere as the official reference for certification and other scheduled performance [10]. By and large, Standard Atmosphere models treat the atmosphere as an ideal gas. Recall that the Earth's atmosphere is a mixture comprised mostly nitrogen (78%) and oxygen (21%). Standard atmosphere models assume air is clean (no dust), dry (no water vapor), and behaves like a perfect diatomic gas, $P = \rho RT$, where P is the atmospheric pressure, ρ is the atmospheric density, T is the absolute atmospheric temperature, and R is the gas constant for dry air.

Reference standard atmospheres [10][11][12] consistently describe the nominal sea-level barometric pressure to be p_0=101,325 Pa (1,013.25 millibars or 2,116.22 lbf/ft^2). This also represents the reading of a Mercury manometer that displays a column 29.92 inches high. Mean sea level is the zero altitude ($h \equiv 0$) for which the initial characteristics (g_o, P_o, ρ_o, T_o) apply on an ideal day.

Some of the other sea-level reference parameters consistent between various atmosphere models [10][11][12] include the sea-level reference density of air: ρ_0 = 1.225 kg/m^3 or 0.0023768 slugs/ft^3, the sea-level reference temperature of air: T_0 = 15 ºC (288.15 ºK or 59 ºF or 518.67 ºR), and the sea-level gravitational acceleration constant: $g0$ = 9.80665 m/s^2 (or 32.17405-ft/s^2).

For practical flight, engineers and pilots need to ensure that aircraft can overfly all terrain and fly at precise enough levels that intersecting routes do not cause random collisions. Because cartographic tradition develops maps with

elevations expressed in terms of height above sea level, aircraft need an **altimeter** to measure their position relative to sea level.

The **geometric altitude**, z, is the measurement that would result if a tapeline could be used to measure the altitude of an object above sea level. In the real world, the variation of gravitational acceleration with latitude, longitude and altitude dependent variation. Some atmosphere models approximate gravitational acceleration, *g(z)*, following the Newtonian inverse square law. They treat the Earth as a non-rotating sphere composed of spherical shells with equal density. g_o is the gravitational constant at sea level and mid-latitude (32.17405-ft/s^2). r_e is radius of earth (approximately 20,855,532-ft).

z is the geometric altitude:

$$g(z) = g_o \left(\frac{r_e}{r_e + z}\right)^2 \tag{14}$$

Thus, in this model the gravitational constant diminishes slightly with increasing altitude.

We may further simplify our analysis by assuming a constant value of gravitational acceleration equivalent to g_o. This results in a measurement known as **geopotential altitude**, h. Because the differences between the geometric and geopotential altitudes vary less than 0.1% for conditions seen during takeoff and landing, we may conflate geometric with geopotential altitude when estimating aircraft performance.

The real atmosphere segregates itself into multiple layers with differing properties.

In the idealized standard atmosphere model, we represent the lowest layer (the tropopause) as a region best modelled as an ideal gas with sea-level temperature, T_o, of 15°C (59°F or 518.67°R) at the reference height, h_o=0-ft, followed by a constant temperature lapse rate, L_o, of -1.9812°C/1,000-ft up to an altitude of h=11 km (36,089-ft). [10][11][12]

$$T = T_o - L_o h = 15^oC - 1.9812^oC \left(\frac{h}{1000\,ft}\right) = 518.67^oR - 3.56616^oR \left(\frac{h}{1000\,ft}\right) \tag{15a}$$

In the idealized world of the standard atmosphere, above the tropopause lies a layer of the atmosphere from 11 to 20 km (36,089 to 65,617-ft) where temperature is invariant with altitude:

$$T = 216.66\ ^oK = 389.99\ ^oR \tag{15b}$$

This layer is the lower stratosphere. Most flight occurs in the troposphere and lower stratosphere. Because the reference atmosphere was defined in metric units, the boundaries between the nominal layers when expressed in feet seem cumbersome and illogical.

A unique relationship exists between the ideal gas law static atmospheric pressure and geopotential altitude. The "Standard Atmosphere" model of static pressure is based upon the density lapse associated with the standard temperature lapse. In the troposphere, i.e. below 36,089-ft:

$$P = P_O \left[1 + \frac{L_o}{T_o} h\right]^{\frac{-g_o}{R L_o}} = 2{,}116.22 \frac{\text{lbf}}{\text{ft}^2} \left[1 + 6.97558E - h\right]^{5.25591} \tag{16a}$$

Whereas in the reference lower stratosphere, above 36,089-ft:

$$P_{tropopause}\, e^{\frac{-g_o}{R T_{tropopause}}(h - h_{tropopause})} = 472.68 \frac{\text{lbf}}{\text{ft}^2} \exp(-4.80637E - 5 * (h - 36089.24)) \tag{16b}$$

where h is the geometric altitude in-ft.

In order for a pilot to infer the vertical position of an aircraft, (s)he will rely upon a static pressure, or manometer, based **altimeter**. Aircraft use pitot-static systems to determine airspeed and altitude. These systems measure total (stagnation) pressure, P_t, and static pressure, P_a. These probes should be designed to be reliable; they must be heated and arranged so that they do not ice over when flying in bad weather or clog from tire splash.

The **altimeter** is a primary device that measures the altitude of an aircraft. Altimeters do not determine height directly; they indirectly infer the altitude by measuring static air pressure. Electronic or mechanical linkages convert the sensed pressure into a **pressure altitude** which can be read by the pilot. Equations 17a and 17b give height as a function of the atmospheric pressure sensed by the altimeter. Equation 17a applies to the notional troposphere and Equation 17b applies to the notional lower stratosphere, where $h_{tropopause}$ is the reference altitude of the tropopause and $p_{tropopause}$ is the static pressure at the tropopause.

$$h = \frac{T_O}{L_O}\left[\left(\frac{P}{P_o}\right)^{\frac{-R\,L_O}{g_O}} - 1\right] \tag{17a}$$

$$h = h_{tropopause} - \frac{R\,T_{tropopause}}{g_o} ln\left(\frac{P}{P_{tropopause}}\right) \tag{17b}$$

Since the real atmosphere does not exhibit precisely the same lapse as the idealized standard atmosphere model, the actual altitude may not correspond the the standard atmosphere calibrated static-pressure derived **pressure altitude**.

In this work we admit that while a reference atmosphere model may serve as a reference, we must ask how well does it represent reality?

Building upon work Sóbester previously published on the problems and perils of stratospheric flight [13], we realized the dearth of recent information documenting the variability of real-world atmospheric conditions expressed in terms that aircraft performance engineers use. In this paper, we compare key climb performance metrics in the synthetic world of the ISA versus real atmosphere equivalents, using historical surface and high altitude observations.

Figure 2 displays historical barometric pressure data for the years 2015 through 2017 for several near-sea-level airports: John F Kennedy in New York City (KJFK), Miami International (KMIA), San Francisco International (KSFO), Amsterdam Schiphol (EHAM) in the Netherlands and Tokyo Haneda (RJTT) in Japan. If we examine this set of surface weather data, we can see that the daily variation in static pressure varies by location: with a 1-standard deviation variation of +/- 1% (+/- 0.3 inHg; or +/- 10 mb) at Schiphol and Heathrow to +/- 0.37% at Miami. We can also see a systematic bias in static pressure. At Miami, the median static pressure has a +0.4% systematic bias (in other words, on an average day at KMIA, *p0* ~ 1,017.30 millibar (2,124.7 lbf/ft^2 or 30.03 inHg) Whereas at Haneda, the median static pressure has a -0.12% systematic bias (in other words, on an average day at RJTT in 2017, *p0* ~ 1016.90 millibar (2,113.7 lbf/ft^2 or 29.88 inHg).

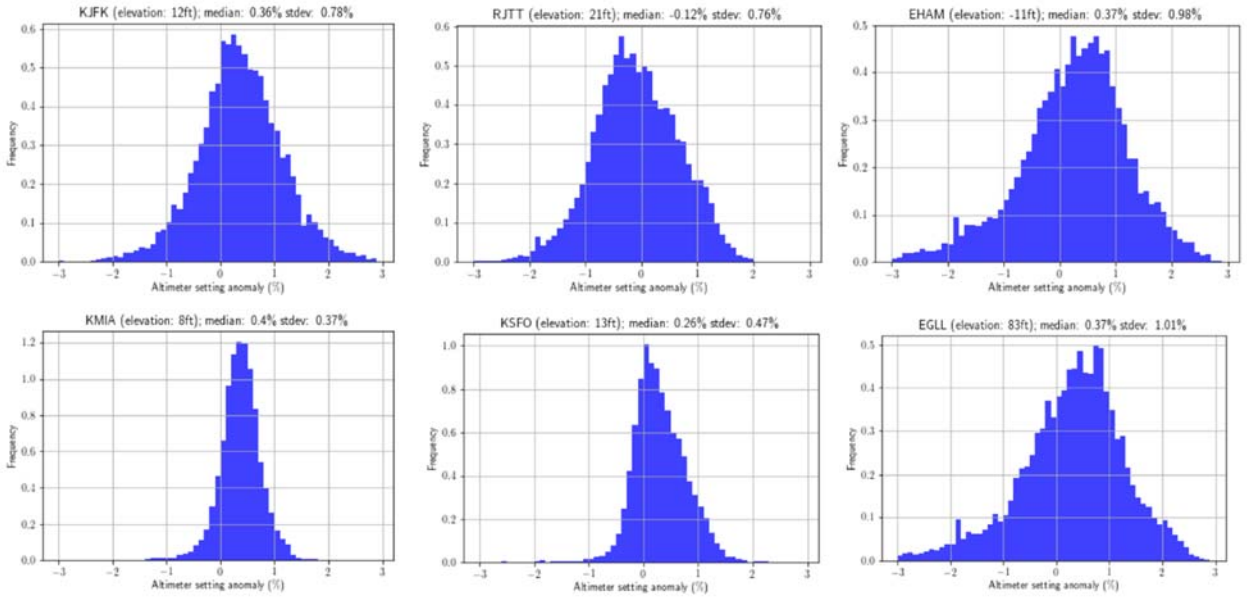

FIGURE 2. METAR Barometric Pressure data from 2015-2017 at several world airports.

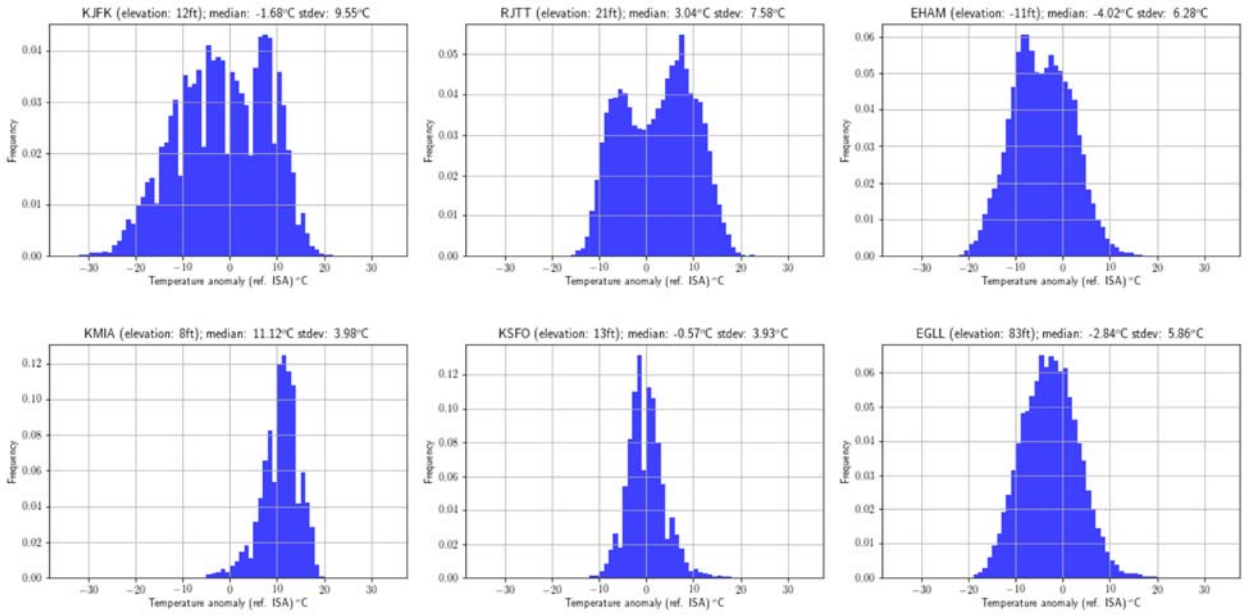

FIGURE 3. METAR Outside Air Temperature data from CY 2015-2017 at several world airports.

We may now turn to Figure 3 which contains historical temperature data for the same collection of airports. All of these airports are essentially at sea level; if the ISA were to literally represent actual conditions they should all report a temperature of ~ 15ºC. However, if we examine this historical surface conditions data set (recorded as METARs at each airport), we can see that the daily variation in temperature varies by location: with a 1-standard deviation variation as high as +/- 9.55ºC (or 3.5% of absolute temperature) at Kennedy. We can also see a systematic bias in ambient pressure. There is a systematic bias of +11.2ºC (4% of absolute temperature) at Miami and -4.02ºC at Schiphol (1.5% of absolute temperature). Because density, viscosity and the local speed of sound are dependent upon the absolute temperature, all of these atmospheric properties relevant to flight may vary when an aircraft departs or lands at a real world airport.

Turning to Figure 4 (overleaf), we can see that in addition to the actual weather being hotter or colder than the reference atmosphere, the actual temperature lapse rate with altitude also varies. Tucson, AZ often exhibits a "temperature inversion", days where the air temperature rises with increasing altitude for the first one thousand or so feet above ground. Buffalo, NY occasionally exhibits a temperature inversion layer for the first five hundred or so feet above ground level. Conversely, Madras, India rarely exhibits a temperature inversion; the temperature almost always decreases as the observer gains height above ground. Aside from the anomalous case of inversions, the tropospheric lapse rate is a lot more consistent than actual temperature values. Overall, all three sites show a trend where temperatures decrease by the time the observer is approximately 2,000 feet above ground.

Turning to Figure 5 (overleaf), we see that a sounding balloon sample from Nottingham, UK closely follows the "standard atmosphere profile" both in terms of sea-level temperatures, the tropospheric temperature lapse rate and the presence of an isothermal lower stratospheric region. In other words, the mean temperature profile at Nottingham from January through December 2017 closely mimics the official 1962 U.S. Standard Atmosphere. [10]

It should be no surprise that real world observational data does not always follow the idealized theory.

Data from Tucson, AZ demonstrates how the tropospheric atmosphere over the American South-West is typically warmer than standard; it also features low altitude temperature inversions followed by a stronger than standard lapse rate of ~ 2.5ºC per 1,000-ft that extends far above the nominal 11 km tropopause level. Madras, India has much less

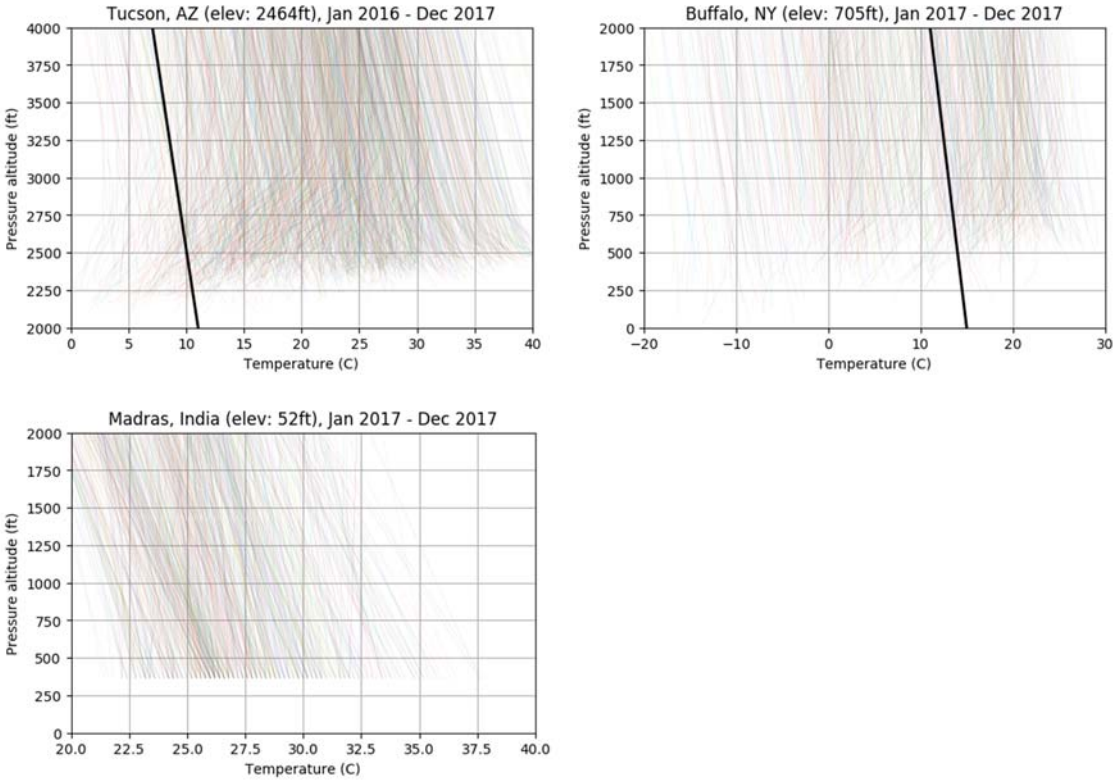

FIGURE 4. Sounding balloon data showing low altitude temperature inversions

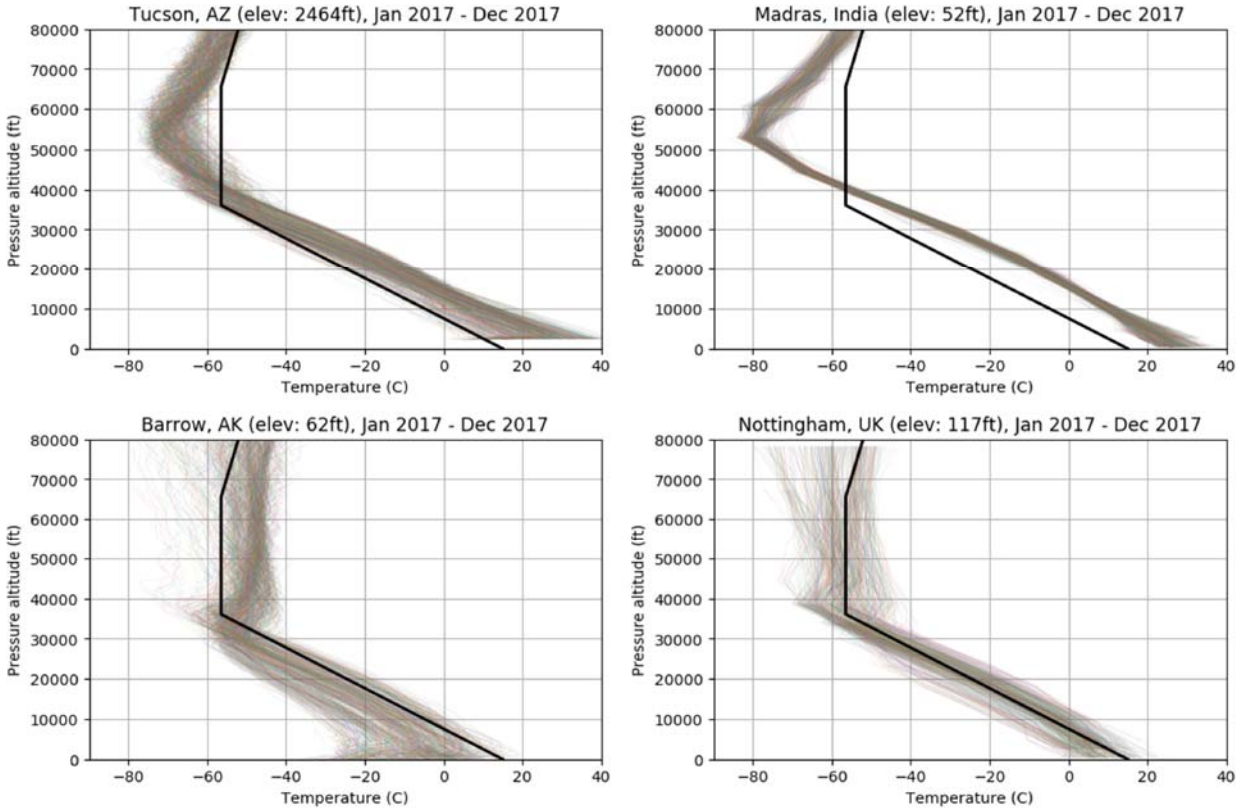

FIGURE 5. Sounding balloon data showing regional variation in altitude/temperature lapse

seasonal variation than Tucson, but shows similar trends: a lapse rate somewhat steeper than the "standard," and the absence of an isothermal lower stratospheric layer. Barrow, AK demonstrates a polar regional characteristic where prevailing sea-level temperatures are colder than the standard followed by a weaker than standard temperature lapse with altitude that transitions at the approximate standard altitude to an isothermal layer that is warmer than the standard.

Thus, we see that the "standard day" model only broadly represents the actual lapse rate at any particular place or time. Figure 5 also shows that the presence of an isothermal layer in the lower stratosphere is both location and season dependent.

Thus, instead of the nominal -1.9812°C/1,000-ft lapse, our Tucson dataset presents a low-altitude temperature lapse of +15°C/1,000-ft and an en-route tropospheric temperature lapse of -2.5°C/1,000-ft.

Similarly, in the Standard Atmosphere tropopause (above 36,089-ft) the temperature lapse declines to zero. In Figure 5 we witness possible lapse rates varying between -2.5°C/1,000-ft (Tucson, AZ) and +2°C/1,000-ft (Barrow, AK and Nottingham, UK).

Later in this work, we will examine the impact of this large discrepancy between the assumed and actual temperature lapse for climb at constant indicated airspeed.

Similarly, the actual pressure lapse rate with altitude does not precisely follow the standard atmosphere model. In Figure 6, using Tucson, AZ as an example, we see that broadly considered measured static pressures track the standard atmosphere profile. But turning to Figure 7 (overleaf), we can see that the actual GPS altitude when compared against the altitude inferred by the reference standard atmosphere model has significant error at typical operating altitudes. For example, at Tucson, AZ there is a daily variation of ~2,000-ft in actual GPS altitude where a standard atmosphere calibrated static pressure altimeter would read 40,000-ft. In addition to the daily variation, we also see a systematic bias present in the data; on average flight at an altimeter reading of 40,000-ft at Tucson, AZ will reflect flight at a true altitude of 41,500 +/- 1,000-ft. Variation is more extreme in Barrow, AK and Nottingham, UK. Variation is greatly reduced in Madras, India. If we compare Figure 7 to Figure 5, we can see that the variation in static pressure lapse does not correlate closely to variation in outside air temperature lapse. Because these variations seem to be largely independent of one another, we can see that a more representative model must take into consideration variation in both temperature lapse and static pressure lapse from the reference standard.

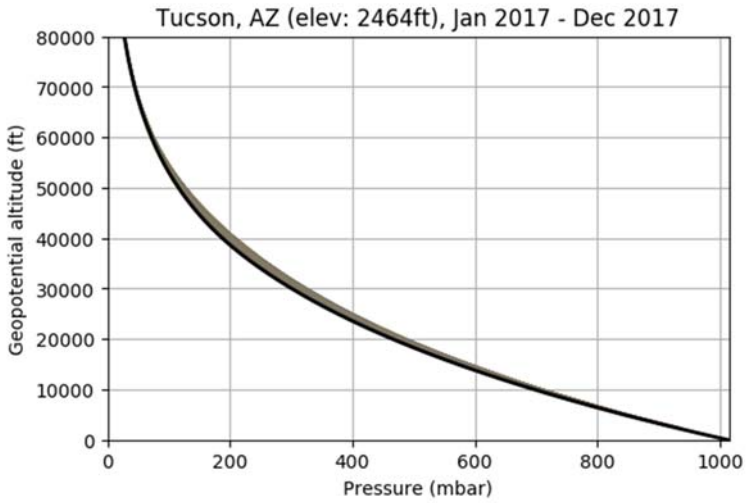

FIGURE 6. Sounding balloon static pressure lapse from Tucson, AZ

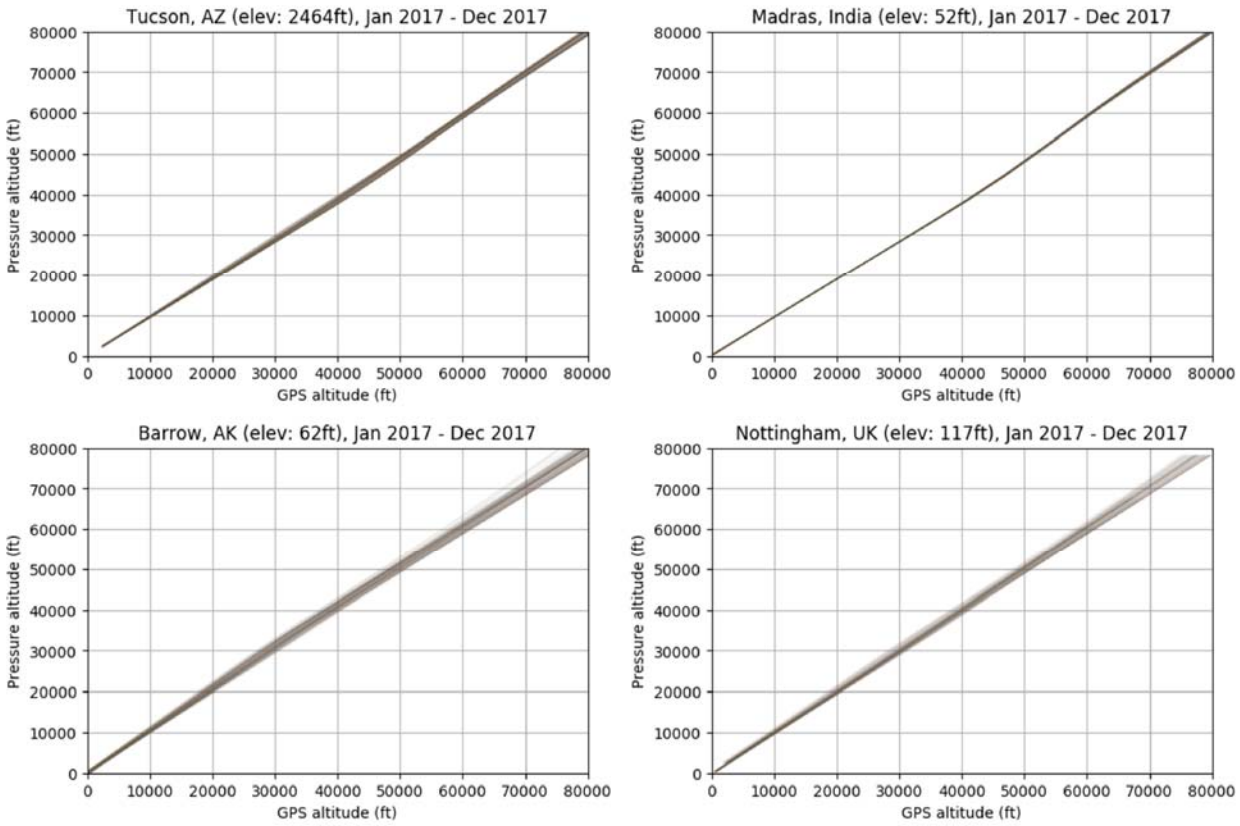

FIGURE 7. Sounding Balloon Data Showing Variation between Actual and Nominal Pressure Altitude derived from the Standard Atmosphere Model.

IV. Aircraft Instrumentation Design & Calibration

Aircraft have successfully flown long before satellite based GPS systems were invented. In this section, we will discuss the sources of error between the sorts of instruments pilots must fly by, and the more "absolute" theoretical models of instrument performance based upon the standard reference altitude.

A. Altimeter Error – Pressure vs Geopotential (Tapeline) Altitude

Recall that the pressure altitude is the geopotential height in a standard atmosphere at which the same pressure occurs. [9] By definition, pressure altitude and geopotential altitude are equivalent in a standard atmosphere and disagree at any given time and place by real world atmospheric effects. Flight levels correspond to the standard-day pressure altitude divided by 100. Thus, flight at a pressure altitude of 32,000-ft is referred to as flight at FL320 ("Flight Level three-two-zero"). If we were to return to our weather balloon and were to examine the actual geopotential altitude (from a GPS) plotted against the inferred pressure altitude (see Figure 9), we would see a general 1:1 correlation but with significant altitude dependent variation. Errors of up to 5,000-ft are indicated in this dataset. Although this error, at first, appears alarming it is of little operational concern so long as all en-route air traffic flies at designated pressure altitude levels (as opposed to GPS altitudes).

Figure 8 (overleaf) highlights a problem that arises on non-standard days. Increments of pressure altitude do not equal increments in geopotential height; thus they introduce error when a performance engineer wants to describe the energy state of the aircraft and estimate climb performance. If we assume the temperature-altitude lapse rate of the standard atmosphere (a big assumption given data shown earlier in this paper), we can estimate the magnitude of this effect:

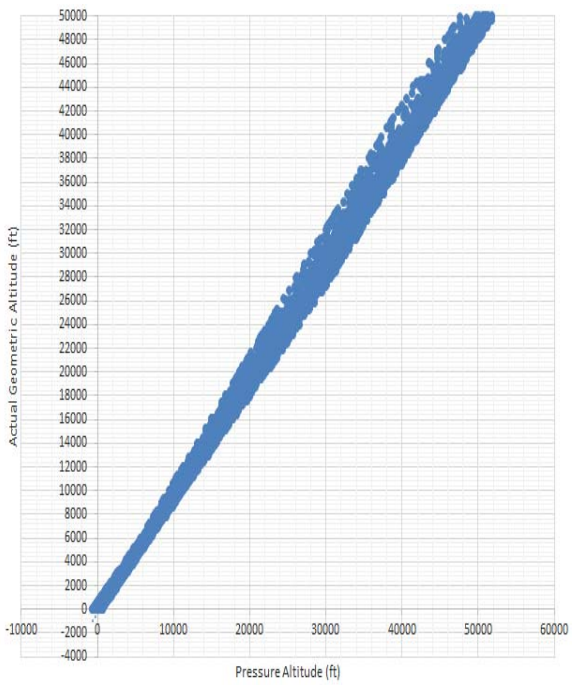

FIGURE 8. The difference between pressure altitude and tapeline altitude as seen in sounding balloon data.

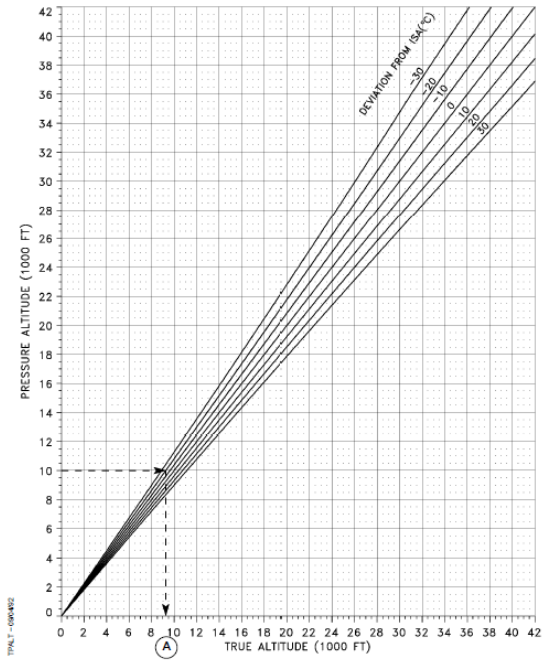

FIGURE 9. **The pressure altitude change associated with a geopotential altitude change when the ambient temperature differs from the standard atmosphere temperature by a constant ISA deviation.** (from Canadair Regional Jet CRJ-900 flight manual) [14]

$$dh = \frac{T}{T_{STD}} dh_P = \frac{T_{STD}+ISAdev}{T_{STD}} dh_P \tag{18}$$

where temperatures are reported in terms of absolute units (Kelvin or Rankine), and the deviation is reported in differential units (ΔCelsius or ΔFahrenheit). Thus for flight near sea level on an ISA+40ºC day (a very hot day seen in desert climates), (TSTD=288.15ºK, ISAdev=+40ºK; T=328.15ºK) **the actual elevation change is ~1.13 times the pressure altitude change**. Similarly on a cold day, the actual elevation change is smaller than the pressure altitude change. Thus the "rate-of-climb" as indicated by differentiating pressure altimeter data will be distorted; on a very cold ISA-40ºC day a manometer based rate-of-climb of 2,000-ft/min climb rate might correspond to an actual climb rate of 1,750-ft/min.

The non-standard-day disconnect between pressure and geopotential altitude may destroy the implicit assumption that cartographic altitudes roughly equal pressure altitudes. Recall there are separate columns for pressure altitude, geopotential and geometric altitudes found in the MIL-STD-3013 polar, tropical and hot day atmosphere models. [10] If we turn to Figure 9, we can see that the effects of weather dependent altimeter error is published as part of the flight manual of a real commercial aircraft (for example, Bombardier's Canadair Regional Jet CRJ-900 [14]). Reading this figure, we see that in order to clear 14,000-ft elevation terrain on an ISA-30ºC day, we would need to schedule flight at or above a pressure altitude of at least 16,000-ft.

B. Airspeed Errors – Indicated vs Calibrated vs Equivalent

Unlike an altimeter, which connects the static source to a sealed bellows, a pitot-static system connects to both the static pressure source and to a total pressure probe. The measured difference between the total and static pressure reflects the magnitude of airspeed (with accuracy that varies with airspeed and altitude).

The Euler equation (Equation 19) applies to steady, inviscid flow along a streamline, and forms the fundamental relationship between airspeed, V, pressure, P, and density, ρ, for all airspeed systems. [16]

$$\frac{dP}{\rho} + VdV = 0 \tag{19}$$

Integrating this equation while assuming adiabatic flow ($\frac{P}{\rho^{\gamma}} = constant$) yields the Bernoulli equation for compressible flow, where γ is the ratio of specific heats for dry air (1.4).

$$\frac{\gamma}{\gamma-1}\frac{P}{\rho}+\frac{V^2}{2}=constant \tag{20}$$

Using the total and static conditions in a pitot-static system (where subscript "*a*" refers to static properties and subscript "*t*" refers to total properties), Equation 20 becomes Equation 21. [16]

$$\frac{\gamma}{\gamma-1}\frac{P_a}{\rho_a}+\frac{V^2}{2}=\frac{\gamma}{\gamma-1}\frac{P_t}{\rho_t} \tag{21}$$

Substituting $\rho_t=\rho_a\left(\frac{P_T}{P_a}\right)^{1/\gamma}$ into Equation 21 yields Equation 22 for V_T, **true airspeed**. True airspeed is usually converted to knots and abbreviated as ***KTAS***. [16]

$$V_T=\sqrt{\frac{2\gamma}{\gamma-1}\frac{P_a}{\rho_a}\left[\left(\frac{P_t-P_a}{P_a}+1\right)^{(\gamma-1)/\gamma}-1\right]} \tag{22}$$

The so-called "compressible q," or q_c, is defined as the difference between the total and static pressures, $q_c=P_t-P_a$ for an ideal Pitot Tube operating in a compressible flow environment. "Compressible q" should not be confused with dynamic pressure, ($q=\frac{1}{2}\rho V^2$), which is different for an incompressible flow.

Calibrated airspeed, Vc, may be thought of in two ways.

An instrument which displays a **reported calibrated airspeed** will present a reading derived from pressures measured by the pitot-static system. It will have corrections applied to best infer the true value of q_c from the measured values. Typically gauges have a fixed calibration made to "best approximate" ideal calibrated airspeed.

United States regulation 14 CFR § 25.1323 (CS 25.1323) establishes permissible inaccuracies in indicated airspeed on transport aircraft. [15] It states that airspeed must be "calibrated to indicate true airspeed (at sea level with a standard atmosphere) with a **minimum practicable instrument calibration error** when the corresponding pitot and static pressures are applied." [15] The overall system error, "that is, the relation between the indicated airspeed and the (ideal) calibrated airspeed in flight and during the accelerated takeoff ground run" must not exceed 3% or 5 *KIAS* through the *critical speed range employed during takeoff and landing flight procedures*. [15] In addition, the pneumatic lines between the pitot-probe and static ports must be short enough that the "effects of airspeed indicating system lag may not introduce significant takeoff indicated airspeed bias, or significant errors in takeoff or accelerate-stop distances." [15] Since most aircraft do not takeoff or land at airspeeds where compressibility effects are significant, it is possible to comply with this regulation with a "calibrated airspeed display" that does not closely match the ideal calibrated airspeed at transonic speeds.

The **ideal calibrated airspeed** may be derived in terms of q_c as:

$$V_{KCAS}=\sqrt{\frac{2\gamma}{\gamma-1}\frac{P_o}{\rho_o}\left[\left(\frac{q_c}{P_0}+1\right)^{(\gamma-1)/\gamma}-1\right]}=\sqrt{7\frac{P_o}{\rho_o}\left[\left(\frac{q_c}{P_o}+1\right)^{2/7}-1\right]} \tag{23}$$

Ideal calibrated airspeed only equals true airspeed at sea-level standard day conditions.

Equation 23 is valid for subsonic flow only. In supersonic flow, a normal shock may be assumed in front of the pitot tube. Herrington [16] uses the Rayleigh supersonic pitot equation to determine airspeeds in a supersonic flow.

By convention, calibrated airspeed is converted to knots and abbreviated as ***KCAS***.

A different version of airspeed termed **indicated airspeed**, V_I, derives from uncorrected (or incompletely corrected) pressure measurements (resulting in an incorrect q_c in Equation 23). Indicated airspeed is customarily displayed in knots and abbreviated as ***KIAS.*** [9] Airspeed systems on older aircraft (and the standby systems used when the primary systems fail on modern aircraft) typically work in indicated airspeed. The displayed value may incur errors

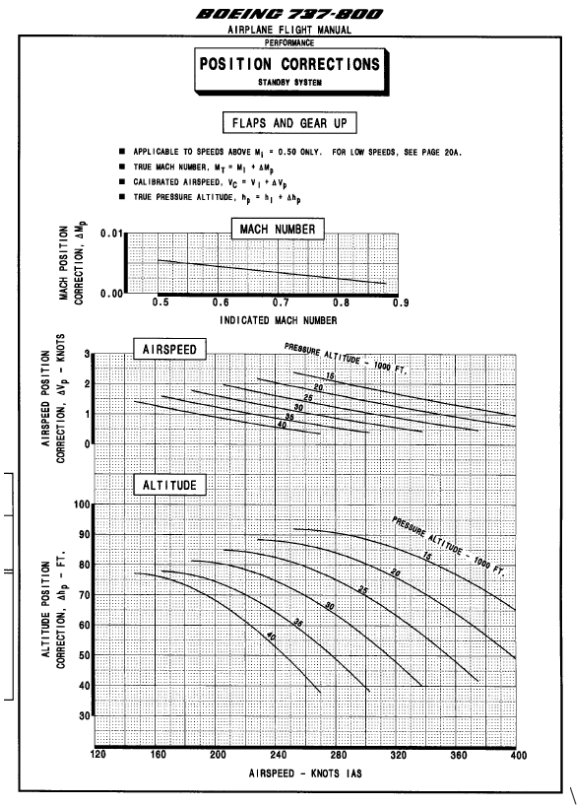

FIGURE 10. Air-data correction table for the standby pitot system. From the flight manual of a B737-800 [17]

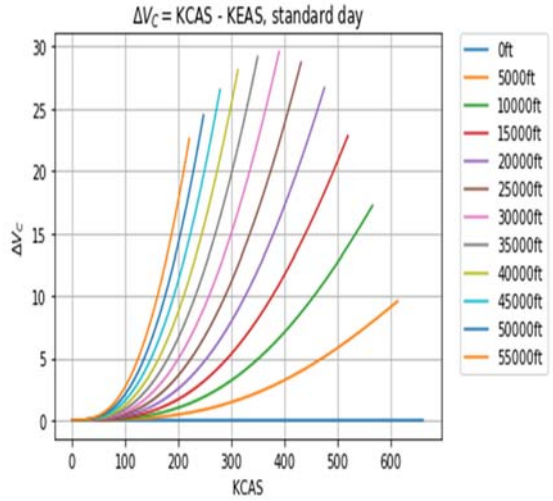

FIGURE 11. Scale-altitude error, V_C - V_E, standard day.

due to the function of the mechanical indicator that, by definition, are *not* part of the indicated airspeed. These **instrument errors** include **scale error**, which results from imperfect mechanization of the controlling equations, as well as other factors such as magnetic forces, friction and the inertia of moving parts. Indicated airspeed (corrected for instrument errors) can be converted to a calibrated value via a correction, ΔV_P, according to Equation 24.

$$(V_C = V_I + \Delta V_P) \qquad (24)$$

Flight manuals (refer to Figure 10) usually provide tables or figures suitable for converting indicated or nominal calibrated airspeeds to ideal calibrated airspeed.

Many engineers work in terms of *KEAS*, which is **knots equivalent airspeed**, an idealized analog of dynamic pressure expressed as if it were airspeed. Equivalent airspeed represents the dynamic pressure formed from flight at that value of nautical miles per hour true airspeed (*KTAS*) under sea-level, standard day conditions. *KEAS* is independent of local atmospheric conditions: temperature, humidity, winds or local barometric variance. To determine dynamic pressure in pounds force per square foot in terms of *KEAS*, engineers may use a modified version of Bernoulli's equation:

$$q = \frac{1}{2}\rho_0 {V_E}^2 = 0.003386 \frac{lbf}{ft^2} KEAS^2 \qquad (25)$$

Rearranging terms, an engineer can infer in terms of practical units the relationship between *KEAS* and dynamic pressure:

$$KEAS = 661.4 \frac{nm}{hr} \sqrt{\frac{q\frac{lbf}{ft^2}}{1481.354 \frac{lbf}{ft^2}}} \qquad (26)$$

Equivalent airspeed serves as a convenient surrogate for dynamic pressure in the structural design of aircraft. Structural limit speeds (limits for things such as flap and landing gear extension) at the design level are often defined in terms of *KEAS*, and then converted to the instrument values (*KCAS* or *KIAS*) when placards and flight manuals are finalized.

The scale-altitude error is the difference between the ideal calibrated airspeed and the equivalent airspeed. It is zero at sea-level and increases with altitude and airspeed, as shown in Figure 11. At the low speeds and low altitudes of airfield performance, the figure shows that the ideal calibrated airspeed is *nearly* equal to equivalent airspeed ($KCAS \approx KEAS$).

Equation 27 presents an approximate correction factor:

$$KCAS \approx KEAS \left(1 + \frac{1}{8}\left(1 - \frac{P(ALT)}{P_0}\right)M^2 + \frac{3}{640}\left(1 - 10\frac{P(ALT)}{P_0} + 9\left(\frac{P(ALT)}{P_0}\right)^2\right)M^4\right) \quad (27)$$

Where P_0 is the static pressure at sea-level standard day, and P(ALT) is the actual at-altitude static pressure.

While many engineers conflate *KIAS*, *KCAS (both "displayed" and "ideal")* and *KEAS*, they do represent distinctly different values; we will need to address these differences when an aircraft flies a constant *KCAS* climb in a real atmosphere.

V. Accelerated Climb Corrections

Returning to the work-energy theorem, we may now apply the lessons learned from studying real-world atmospheric models and real-world aircraft instruments to address the necessary corrections to estimate the rate-of-climb of an aircraft under constant indicated airspeed and/or constant Mach number conditions. In this section we will identify the "correction" terms necessary to consider:

1. Low-altitude climb at constant indicated airspeed (typically under 250 *KIAS*) on a cold day (where the reported pressure altitude does not agree with the tapeline altitude)
2. Constant calibrated airspeed (*KCAS*) or constant Mach number climb around 30,000-ft (troposphere) where the airspeed compressibility correction cannot be neglected
3. Constant calibrated airspeed (*KCAS*) or constant Mach number climb around 30,000-ft (troposphere) where the temperature lapse deviates from the standard

A. Error Associated with the Disconnect between the Tapeline Altitude and Pressure Altitude

Any errors arising from the disconnect between the actual, "tapeline" altitude and the pressure altitude will manifest themselves as an error in the displayed altitude of a classic static pressure altimeter. In addition, a classic static pressure based "rate-of-climb" instrument will present an inaccurate reading. However, physics-based simulations based upon accurate aerodynamic, atmospheric and propulsion models will properly model aircraft motion. Thus, while an instrument might indicate a 500-ft/min climb rate; a physics-based that captures the true equations-of-motion will predict the actual climb rate provided that the underlying atmosphere and propulsion models consider the actual tempertature and density lapse rate and the aerodynamic model properly accounts for both Mach and Reynolds Number dependencies in coefficient data.

B. Accelerated Climb Derivation

Roskam [2] presents the classical derivation to find the correction factor for accelerated climbs.

$$K_{accel} = \frac{1}{\left(1 + \frac{V_{KTAS}}{g}\frac{dV_{KTAS}}{dh}\right)} = \frac{1}{\left(1 + 0.088465\, KTAS\frac{dKTAS}{dh}\right)} \quad (28)$$

Thus for each case (constant *KEAS* or Mach) climb, we need to determine the value of *KTAS* and d*KTAS*/dh (in nM/hr/ft) as appropriate for the circumstances.

For climb at constant equivalent airspeed (*KEAS*), following Equations 27 and 28, we see that the relationship between the true airspeed and the equivalent airspeed is a function of the density of the air.

$$KEAS(ALT) = KTAS\sqrt{\frac{\rho(ALT)}{\rho_0}} \quad (29)$$

or

$$KTAS(ALT) = KEAS\sqrt{\frac{\rho_0}{\rho(ALT)}} \quad (30)$$

Thus we may write the derivative (following the chain rule) as:

$$\frac{dKTAS}{dh}(ALT) = \frac{1}{2} KEAS \left(\frac{\rho(ALT)}{\rho_0}\right)^{\frac{3}{2}} \frac{1}{\rho_0} \frac{d\rho(ALT)}{dALT} \tag{31}$$

Further substitution results in the following relationship for climb at constant calibrated airspeed:

$$KTAS(ALT) \approx \frac{KCAS}{1+\frac{1}{8}\left(1-\frac{P(ALT)}{P_0}\right)M^2+\frac{3}{640}\left(1-10\frac{P(ALT)}{P_0}+9\left(\frac{P(ALT)}{P_0}\right)^2\right)M^4} \sqrt{\frac{\rho_0}{\rho(ALT)}} \tag{32}$$

We must also remember that the Mach number is related to the true airspeed through the speed of sound:

$$KTAS = M \cdot a = M \cdot a(ALT) \cdot \left(\frac{3600\ sec/hr}{6076.12\ ft/nM}\right) \tag{33}$$

Where the speed of sound is proportional to the square root of the air temperature:

$$a(ALT) = 1116.45 \frac{ft}{sec} \sqrt{\frac{\mathrm{T}(ALT)\ ^\circ R}{518.67\ ^\circ R}} \tag{34}$$

$$M = \frac{V_{KTAS}}{a(ALT)} = \frac{V_{KTAS} \cdot \left(\frac{3600\ sec/hr}{6076.12 \frac{ft}{nM}}\right)}{1116.45 \frac{ft}{sec} \sqrt{\frac{\mathrm{T}(ALT)\ ^\circ R}{518.67\ ^\circ R}}} \tag{35}$$

Hence, we must solve by relaxation, the values of true airspeed Equation 33 when combined with Equation 35.

We then must differentiate these results to obtain d*KTAS*/dh for climb at constant calibrated airspeed.

C. Standard Day Correction Factors

Our numerical solutions of the *"K"* factors for constant Mach number and constant *KEAS* climb matches the Ref 8 expressions within +/- 0.01% .

On a standard day, a real climb flown at constant *KCAS* (as opposed to constant *KEAS*) will exhibit some slight variation. If we consider an aircraft that climbs from sea level to 50,000-ft at a constant ideal calibrated airspeed, we will see that this represents a flight where the equivalent airspeed decreases slightly as the altitude increases; see Figure 13. This represents the effect of Equation 29, which is purely a function of Mach number.

Note that 250-*KCAS* represents flight at Mach=0.377 at sea-level and Mach ~ 1 at 49,000-ft.

Because the equivalent airspeed (see Figure 13, overleaf) and true airspeed (see Figure 14, overleaf) decline more rapidly with altitude as an aircraft follows a 250-*KCAS* (as opposed to 250-*KEAS*) climb, the aircraft will exchange additional kinetic energy into potential energy. An aircraft will climb more strongly than its predicted unaccelerated rate-of-climb-rate when it needs to lose kinetic energy to maintain a given speed schedule.

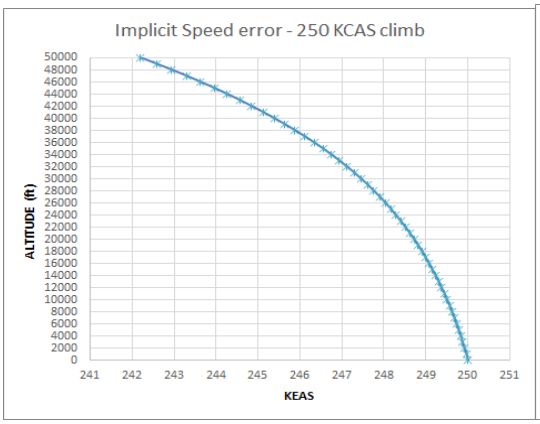

FIGURE 13. Equivalent airspeed as a function of altitude for climb at 250-*KCAS*; ISA standard day.

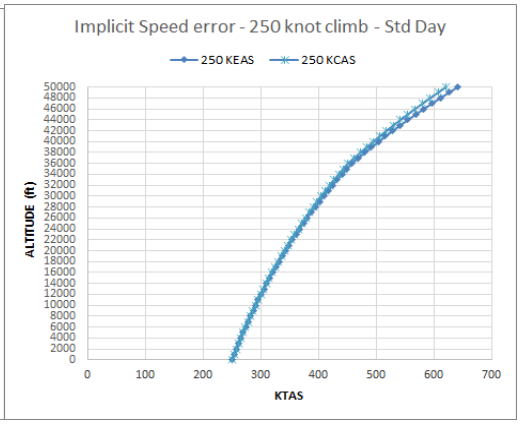

FIGURE 14. True airspeed as a function of altitude for climb at 250-*KCAS*; ISA standard day.

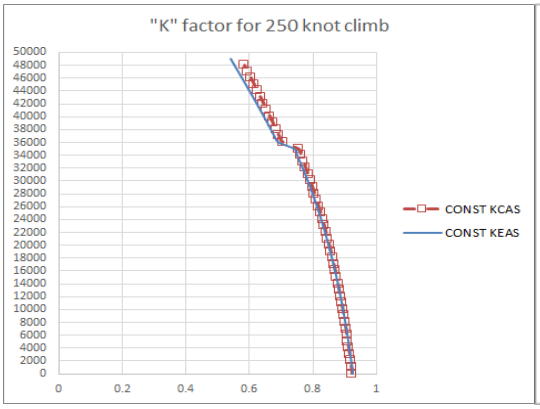

FIGURE 15. *"K"* factor as a function of altitude for 250-*KEAS* and 250-*KCAS* climb; ISA standard day.

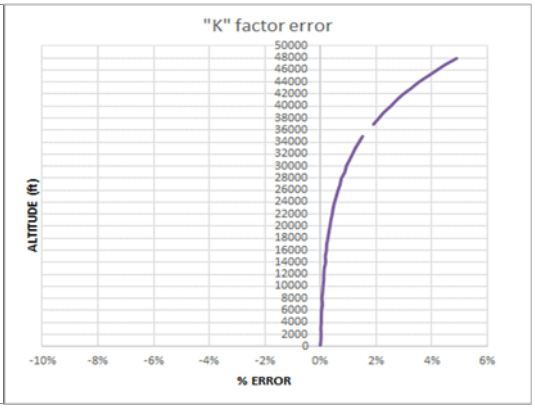

FIGURE 16. Error in *"K"* factor for 250-*KCAS* climb modelled as a 250-*KEAS* climb; ISA standard day

As a consequence of this, we see in Figure 15, that the *"K"* factor for a constant *CAS* climb is consistently larger than the *"K"* factor for a constant *EAS* climb.

Figure 16 reveals that the standard day *"K"* factor for *EAS* climb underpredicts the actual ideal *CAS* climb performance by up to 5%. The error is less than 1% up to 30,000-ft, but grows larger at higher altitudes.

D. Constant ISA Deviation Correction Factors

We now turn to numerical solutions of the *"K"* factors for constant Mach number and constant *KEAS* climb for non-standard days but with constant temperature offset. On a uniformly hot day (where the ISA deviation is constant with increasing altitude), the air densities are lower and the speed of sound higher than represented by the ISA standard atmosphere.

Our numerical solutions for *"K"* factor for constant Mach number climb reveal that the change in speed of sound due to elevated temperatures offsets the reduction in air density. While density effects upon hot-day engine performance may reduce the unaccelerated climb performance, the *"K"* factor remains unchanged as an increase in temperature reduces the *KTAS* which exactly cancels the increase in d*KTAS*/dh. Thus, Blake's [8] formulas for *"K"* appear to be derived for a climb at constant ISA deviation.

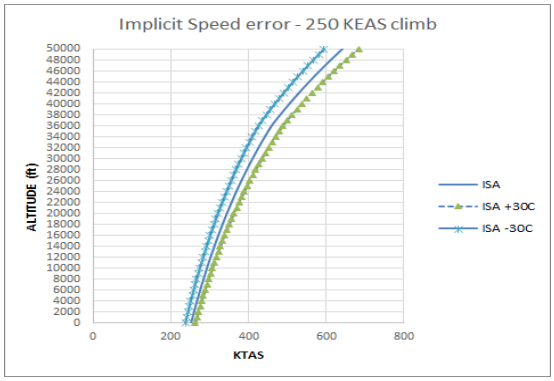

FIGURE 17. True airspeed as a function of altitude for climb at 250-*KEAS*; non-standard day.

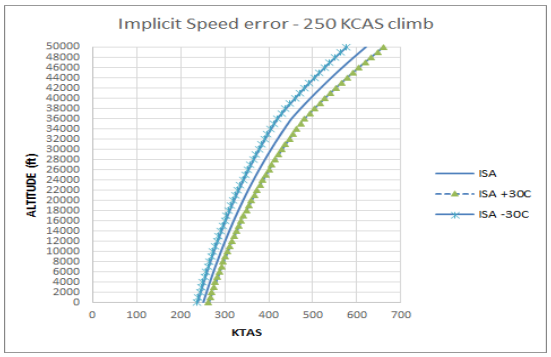

FIGURE 18. True airspeed as a function of altitude for climb at 250-*KCAS*; various temperatures.

Our numerical solutions for *"K"* factor for constant *EAS* climb show a strong temperature dependence in true airspeed; see Figure 17. As the weather grows warmer than standard day, the air density at any given altitude decreases. This causes an increase in true airspeed at equivalent *KEAS*.

Similarly, the numerical solutions for *"K"* factor for constant *CAS* climb show a similarly strong temperature dependence in true airspeed; see Figure 18. As the weather grows warmer than standard day, the air density at any given altitude decreases. This, along with the application of the scale-altitude correction, causes similar increases in true airspeed with increasing altitude at a constant *KCAS*.

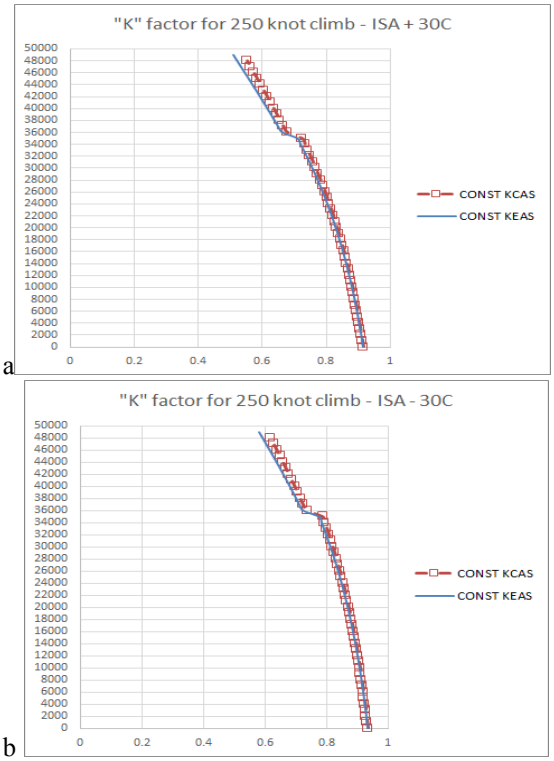

FIGURE 19. *"K"* factor for climb at 250-*KEAS* and 250*KCAS* on ISA+30C and ISA-30C days.

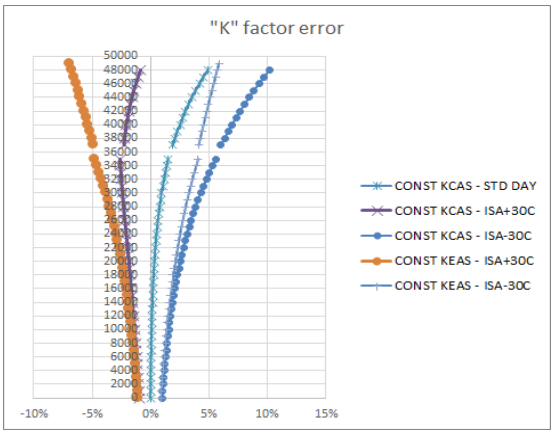

FIGURE 20. Error in *"K"* factor for 250-*KCAS* and 250-*KEAS* climbs on non-standard days with climb modelled as a 250 *KEAS* standard day climb

Figure 19 shows how much the *"K"* factor varies with temperature; for constant *EAS* climb we see at 40,000-ft that k=0.646 on a standard day, k=0.616 on an ISA+30°C day and k=0.679 on an ISA-30°C day. This represents a potential +/- 5% error in *"K"* factor due to local weather, above and beyond the variation in inherent climb performance due to changes in air temperature and density.

Turning to Figure 20, we see that the error associated with using the standard day constant *EAS* climb correction to represent constant *EAS* climb on non-standard days may exceed 5% at 40,000-ft. The error associated with using the standard day constant *EAS* climb correction to represent constant *CAS* is even worse on cold days. Under typical conditions, such as a 250-*KCAS* climb at 30,000-ft we see a +2/-4% variation in *"K"* factor from the notional 250

KEAS climb performance. Again, this is above and beyond any changes in propulsive thrust arising from changes in outside air temperature and density.

E. Comparison of Real Atmosphere with Standard Day Factors

In Figure 21, we can examine the difference in altitude dependent atmospheric properties in comparison with the ISA standard day model. Here, we plot measured temperatures at Barrow, AK, Buffalo, NY, Tucson, AZ, Madras, India and Nottingham, UK as a function of altitude. We selected the particular days to highlight weather conditions that lead to large discrepancies with the standard day model. Tucson, in January, closely follows the standard day. Barrow exhibits considerable variation in the temperature lapse rate with increasing altitude. Barrow and Nottingham lack an isothermal break in the tropopause. Madras is both much warmer than standard; the stratospheric break occurs above the 40,000-ft limit of this plot.

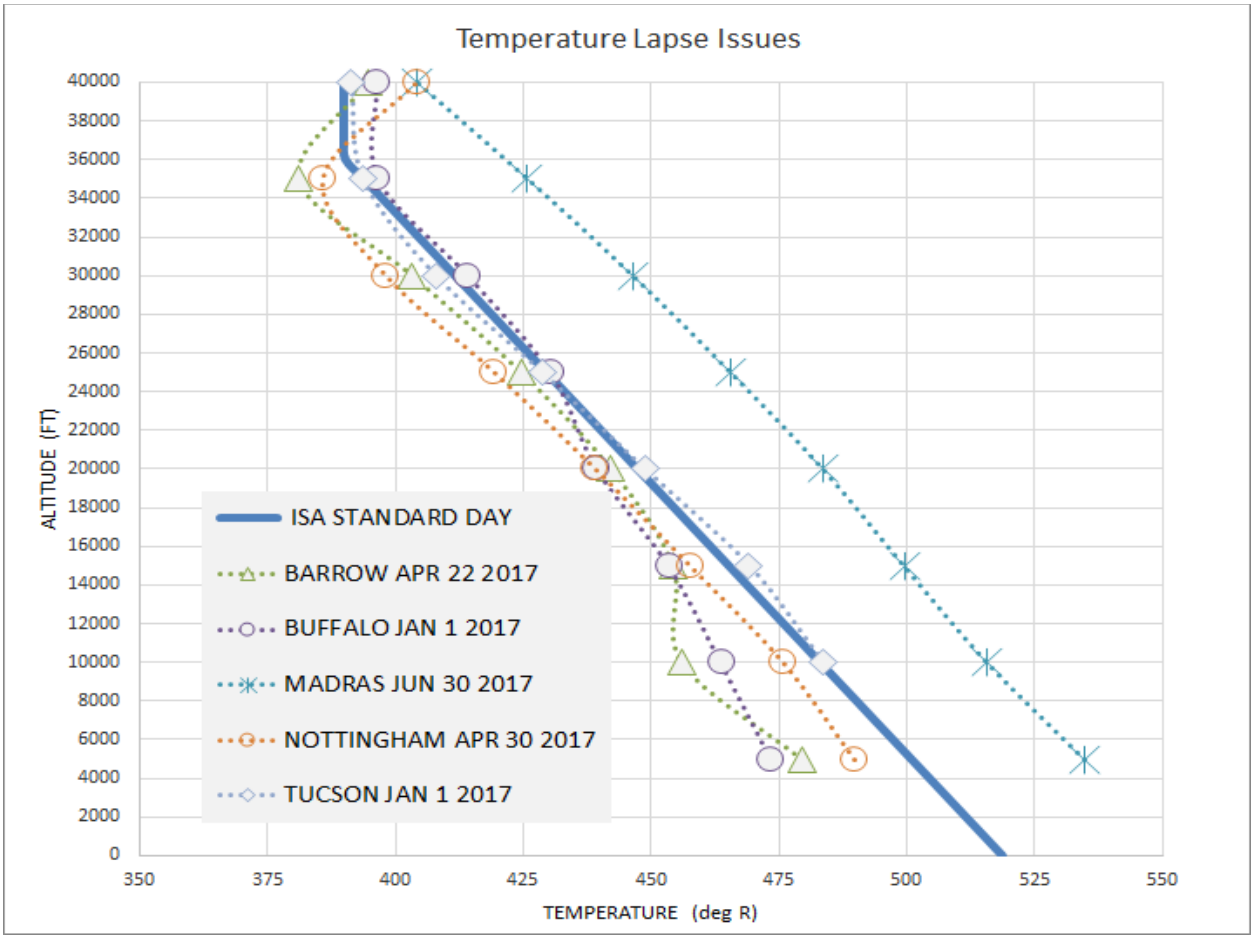

FIGURE 21. Temperature Lapse (real world weather compared to theoretical standard-day ISA model)

We can infer from the reported temperature and pressure profiles the speed of sound (see Figure 22, overleaf) and density (see Figure 23) lapse as a function of altitude. From these values, we can then infer the true airspeed (see Figure 24, subsequent pages) and from this the true airspeed lapse rate for a climb at various conditions. In Figure 25, we present the *"K"* factor from Equation 30 determined using actual measured atmospheric properties alongside the standard day Blake [8] formula for constant *EAS* climb, and our estimates of constant 250-*KCAS* climb shown earlier in the manuscript.

Figures 25 and 26 (subsequent pages) reveal that that the real-world true airspeed lapse with altitude results in variations in *"K"* factor that swamp the difference between the standard-day *EAS* and *CAS* predictions. Compairing the two figures (250-*KCAS* and 300-*KCAS*) with one another, we can see that the implicit error that arises when one conflates a typical constant *CAS* climb with the *EAS* correction grows as the scheduled climb speed increases.

Consider the implications in the "real world."

In our first hypothetical case, you are trying to climb at 250-*KCAS* at 35,000-ft. According to the simple Reference 8 formula (conflating *KEAS* and *KCAS*), k=0.7432. In a perfect ISA world, *k* would be 0.7522 (a 1.1% discrepancy) when accounting for the difference between *EAS* and *CAS*. However, under actual weather conditions both the true airspeed and true airspeed altitude lapse rates vary widely from that implied by the ISA model: at Barrow that would be k=0.657, Buffalo k=0.689, Madras k=0.764 , Nottingham k=0.631and Tucson k=0.700. If the engineer knows the correct ISA-deviation weather and have the appropriate aerodynamic and propulsive models along with the weight, and climb speed (*KCAS*), a model assuming ISA based k-factors might predict a 500-ft/min climb rate while the actual aircraft might exhibit anywhere from 424-ft/min (Barrow) to 514-ft/min (Madras).

In our second hypothetical case, you are trying to climb at 300-*KCAS* at 25,000-ft. According to the simple Reference 8 formula (conflating *EAS* and *CAS*), k=0.7609. In a perfect ISA world, k would be 0.7587 (a negligible 0.3% discrepancy) when accounting for the difference between *KEAS* and *KCAS*. However, under actual weather conditions both the true airspeed and true airspeed altitude lapse rates vary widely from that implied by the ISA model: at Barrow that would be k=0.7607, Buffalo k=0.7444, Madras k=0.773, Nottingham k=0.7562 and Tucson k=0.7607. Here, a model assuming ISA based k-factors might predict a 2000-ft/min climb rate while the actual aircraft might exhibit anywhere from 1950-ft/min (Barrow) to 2030-ft/min (Madras). The errors are not large, but they are noticeable.

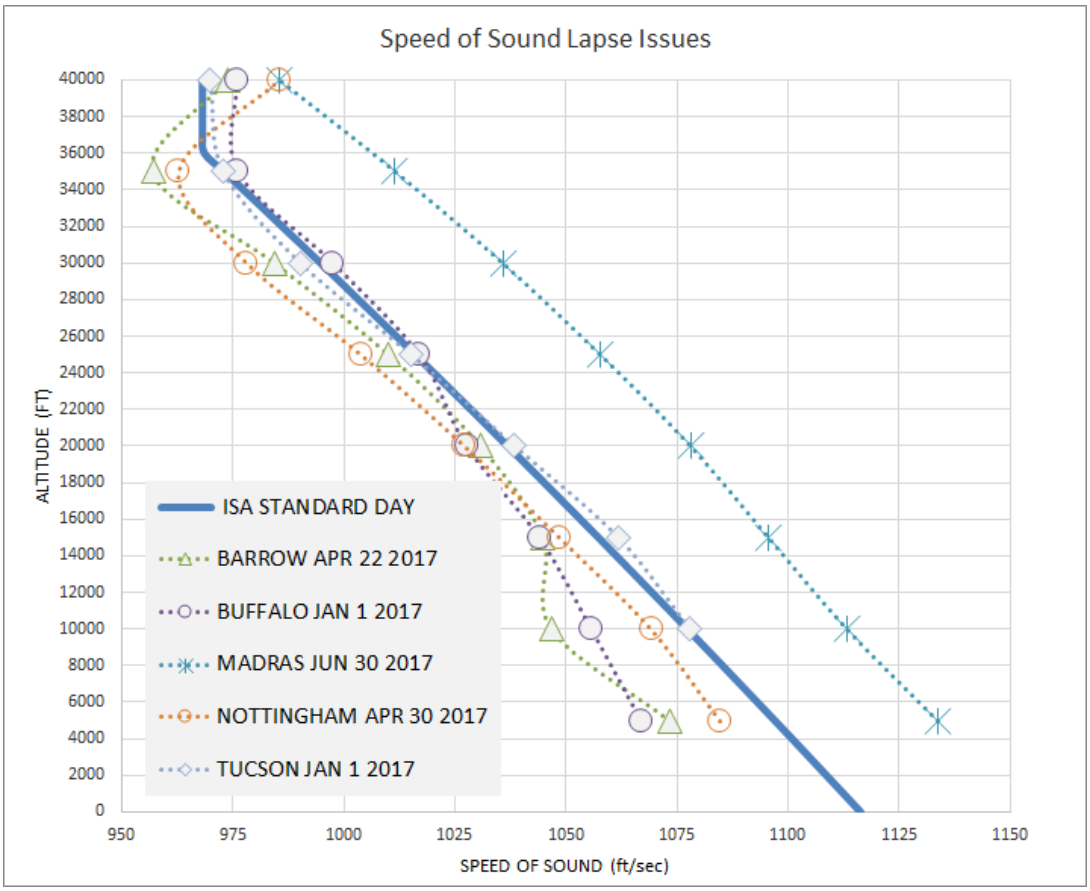

FIGURE 22 – Speed of sound lapse (real world weather compared to theoretical standard-day ISA model)

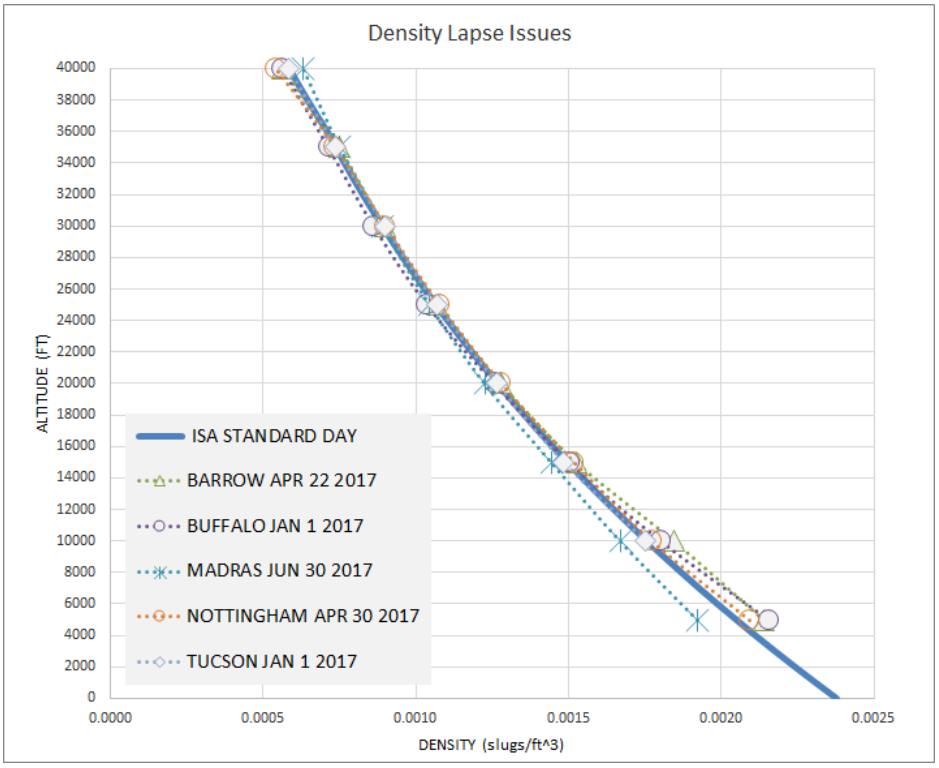

FIGURE 23 Density lapse (real world weather compared to theoretical standard-day ISA model)

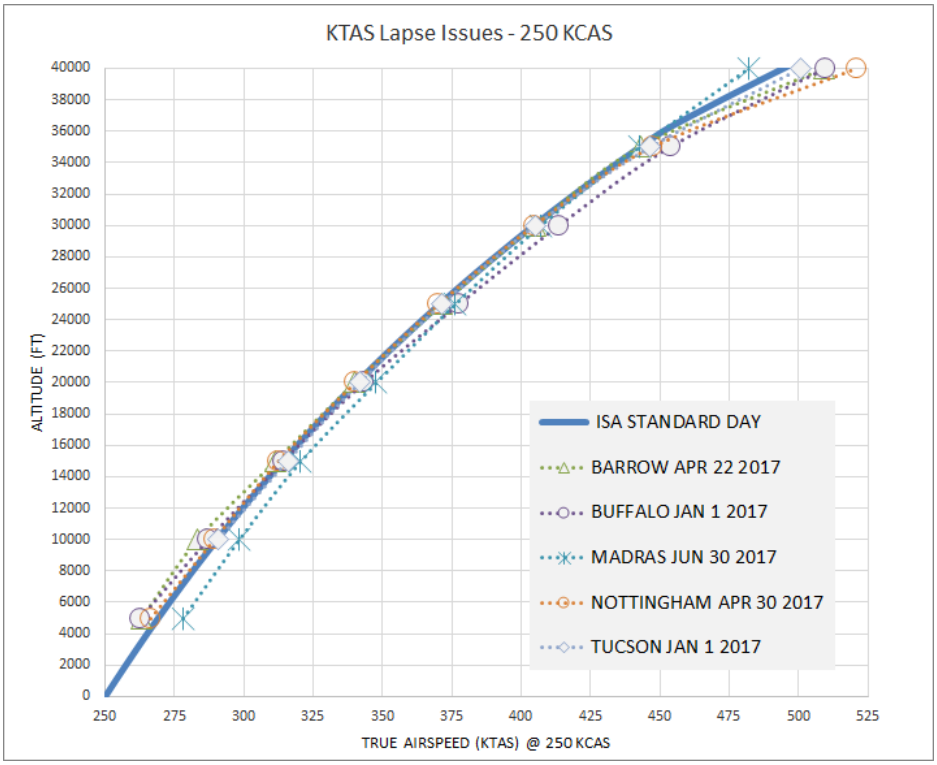

FIGURE 24 - *KTAS* lapse rate @ 250-*KCAS* (real world weather compared to theoretical standard-day ISA model)

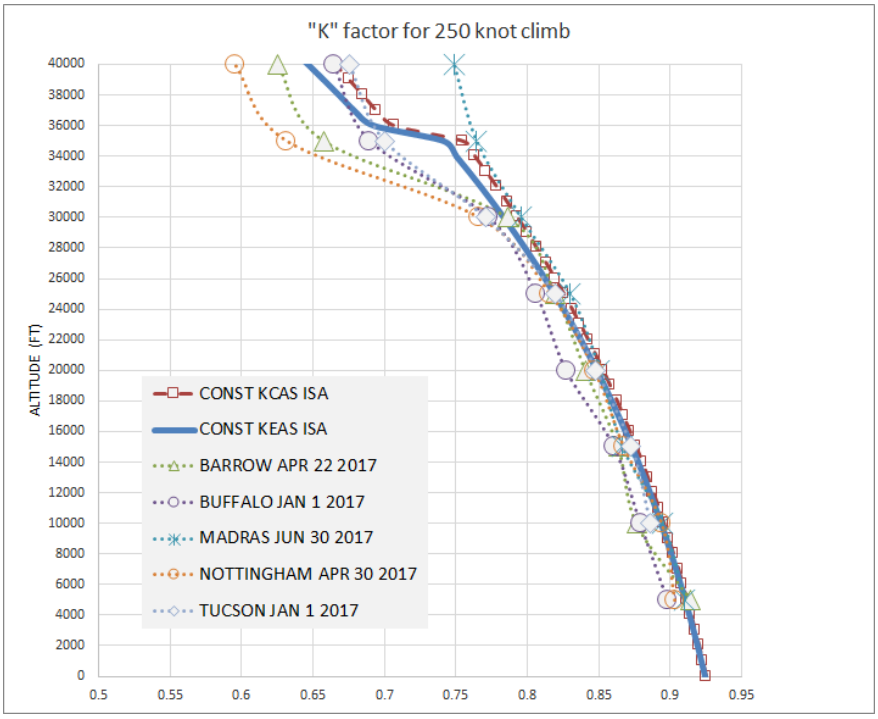

FIGURE 25 - *"K"* factor for 250 knot climb (const CAS under real world weather compared to theoretical constant CAS and constant EAS)

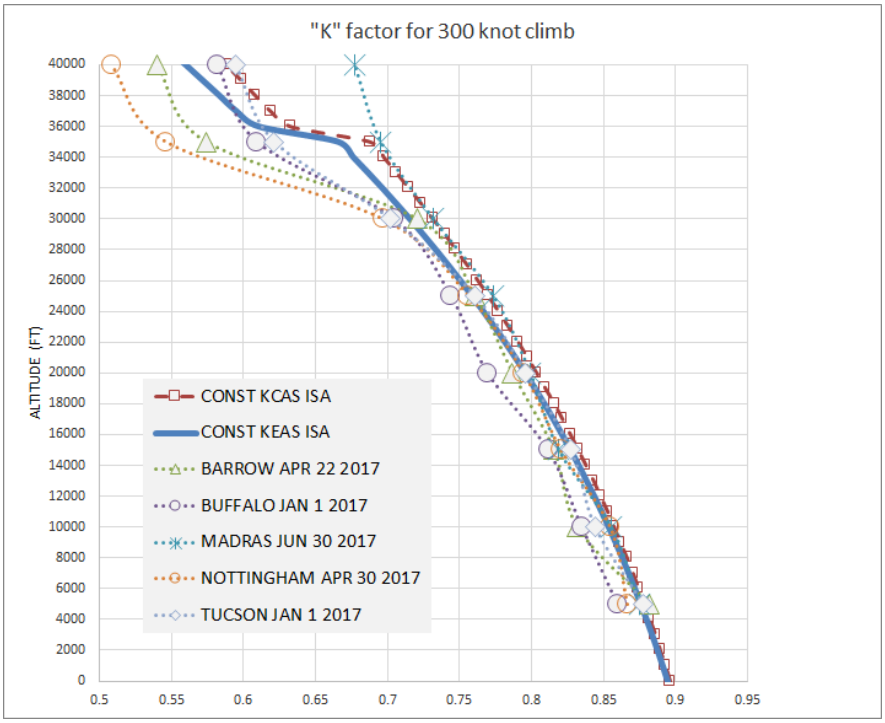

FIGURE 26 - *"K"* factor for 300 knot climb (const CAS under real world weather compared to theoretical constant CAS and constant EAS)

VI. Reccomendations and Conclusions

In summary, we observed the following:

1. The basic unacelerated climb performance can not be accurately modelled using the work-energy theorem; this is the take-away from Takahashi [5].

2. In all cases, the thermodynamic engine model must take into account the changes in thrust and thrust-specific-fuel-consumption of the engine flown in weather warmer or cooler than the standard.

3. Low-altitude climb at constant indicated airspeed (typically under 250 *KIAS*) on a cold day (where the reported pressure altitude does not agree with the tapeline altitude) requires the pilot to understand that the rate-of-climb indicator dial will report a lower rate of climb than the aircraft actually attains; in other words the indicator might read 2,000ft/min when the actual airplane is ascending at 2,100-ft/min. Thus, the actual climb gradient capability does not degrade under these circumstances.

4. Constant calibrated airspeed climb around 30,000-ft (troposphere) where the airspeed compressibility correction cannot be neglected introduces a 1% error in *"K"* factor from a constant equivalent airspeed climb. This error increases substantially in the event that the aircraft is flying under non-standard conditions. The error due to temperature deviation seems to be larger than the temperature due to changes in lapse rate. On an ISA+30C day the *"K"* factor is 2% optimistic; the real aircraft will climb more slowly at constant *CAS* than it would if flown at constant *EAS*.

5. The premature, delayed presence or absence of the iso-thermal stratospheric zone leads to large changes in both temperature deviation and temperature lapse rates. These effects combine to render the at-altitude climb performance *"K"* factor substantially different than the nominal equation. We see a 20% error present (refer back to Figure 25) in constant EAS rate-of-climb *"K"* factors through the mid-30,000 fts.

6. Temperature effects do not seem to impact the constant Mach *"K"* factors. Still, the climb performance will vary with outside temperature because propulsive thrust at altitude will due to temperature deviation driven changes in air density.

Thus, we believe that these otherwise overlooked factors need to be considered in conceptual design, detail design as well as production flight-test-data-reduction and flight manual phases of any major aircraft project. Future work will examine how does all this play out with the response of the propulsion system and commonly used propulsion models to the same differences in atmospheric properties and lapse rates.

References

[1] Anderson, J.D., *Aircraft Performance and Design*, McGraw-Hill, New York, 1999.
[2] Roskam, J. and Lam, C., *Airplane Aerodynamics and Performance*, DAR Corporation, Lawrence, KS, 1997.
[3] Raymer, D.P., *Aircraft Design: A Conceptual Approach*, AIAA, Washington DC, 1989.
[4] Nicolai, L.M., *Fundamentals of Aircraft Design*, METS, San Jose, CA, 1984.
[5] Takahashi, T.T., "A Bad Moon Rising: The Puzzling Inaccuracies of the Work-Energy Theorem in Aircraft Performance," AIAA 2019-1305, 2019.
[7] DeBothezat, G., "General Theory of the Steady Motion of the Airplane," NACA TR-97, 1921.
[8] Anon., *Jet Transport Performance Methods*, Boeing Flight Operations Engineering Training Document D6-1420, 7th Edition, Boeing, Seattle, WA, May 1989.
[9] 14 CFR 1.1 "General Definitions," (2018)
[10] U.S.Standard Atmosphere, 1962, U.S. Government Printing Office, Washington, D.C., 1962
[11] Manual of the ICAO Standard Atmosphere (extended to 80 kilometres (262 500 feet)) (Third ed.). International Civil Aviation Organization. 1993. ISBN 92-9194-004-6. Doc 7488-CD.
[12] MIL-STD-3013 Revision A, GLOSSARY OF DEFINITIONS, GROUND RULES, AND MISSION PROFILES TO DEFINE AIR VEHICLE PERFORMANCE CAPABILITY, September 9, 2008.
[13] Sóbester, A. *Stratospheric Flight: Aeronautics at the Limit*, Springer-Praxis, New York, 2011.

[14] CRJ705/900 Flight Planning and Cruise Control Manual, CSP C-118, Bomardier, Montreal, QC, Canada (dated Apr 21/2006)
[15] 14 CFR § 25.1323
[16] Herrington, R.M. "USAF Flight Test Engineering Manual," Air Research & Development Command, Edwards AFB, Edwards, CA,
[17] B737-800 Airplane Flight Manual (AFM), Boeing Commercial Airplane Group, Seattle, WA.
[18] Engineering Sciences Data Unit, "Acceleration factors and descent rates at constant EAS, CAS, M", ESDU Data Item No. 81046, Issued November 1901, with Amendment A, June 1992.
[19] Engineering Sciences Data Unit, "Effects of small changes on rate of climb", ESDU Data Item No. 94039, Issued October 1994.
[20] Engineering Sciences Data Unit, "Estimation of rate of climb", ESDU Data Item No. 92019, Issued June 1992.